

OPTIMISATION OF HYBRID MICROCHANNEL HEAT SINK WITH
SECONDARY CHANNEL UNDER LAMINAR FLOW CONDITION

WAN MOHD. ARIF BIN AZIZ JAPAR

UNIVERSITI TEKNOLOGI MALAYSIA

OPTIMISATION OF HYBRID MICROCHANNEL HEAT SINK WITH
SECONDARY CHANNEL UNDER LAMINAR FLOW CONDITION

WAN MOHD. ARIF BIN AZIZ JAPAR

A thesis submitted in fulfilment of the
requirements for the award of the degree of
Doctor of Philosophy

Malaysia-Japan International Institute of Technology
Universiti Teknologi Malaysia

JULY 2022

DEDICATION

This thesis is dedicated to my lovely parents, who always support me, uplift me, comfort me, and bring joy to my soul during my difficult time. It is also dedicated to my best friend, who supports me, helps me, listens to everything I say, and does not judge me.

ACKNOWLEDGEMENT

First and foremost, all Praise to Allah S.W.T the Almighty, for giving me the blessing, health, patience, knowledge, endurance, chance and strength to complete this research. Thank Allah for sticking by my side when I felt like I was drowning in a sea of sorrow during my study. There are no words that can express my gratefulness and appreciation to Him in the whole process of writing, compiling and preparation of this thesis. Thank Allah for everything that I have.

This PhD journey would not have been possible without the support of my lovely family, dedicated supervisors, supportive colleagues and friends. I would first like to express my sincere appreciation towards my father, Aziz Japar Bin Osman. He is the strongest person in my life. In my fourth semester, he was diagnosed as having heart disease. At first, I want to stop my study so that I can help my family. But he disagreed with my decision and asked me to continue my study. He believed in me and wanted the best for me. Besides that, I would like to thank my lovely mother, Raja Alizah Binti Raja Lon, for her emotional and moral support throughout my PhD journey.

I would like to acknowledge and thank my supervisors, Associate Professor Dr. Nor Azwadi Che Sidik, Dr. Natrah Kamaruzaman and Professor Dr. Saidur Rahman, for guiding me to conduct my research and providing any assistance requested. All of them have given generously of their expertise, time and energy, and I am richer for it. Associate Professor Dr. Nor Azwadi Che Sidik and Professor Dr. Saidur Rahman help me a lot in the numerical analysis and writing skills. In contrast, Dr. Natrah Kamaruzaman helps me in the experimental setup and design. Combination of their expertise has made this research has progressed well as planned, however, some of the activities were affected during Covid-19 pandemic. I really appreciate their help during the Covid-19 pandemic. We have worked together to ensure other plans can still be continued during the Covid-19 pandemic. Besides that, I would like to thank Professor Dr. Yutaka Asako, who always helps me to overcome all the obstacles via his encouragements and comments.

I would like to express my deepest gratitude to Malaysia-Japan International Institute of Technology (MJIIT), Universiti Teknologi Malaysia (UTM) for providing Doctoral scholarship for my study. Besides that, I would like to thank Takasago Thermal Engineering Co. Ltd., Japan, for providing research funding to this project.

Finally, I would like to thank my best friend, Mr. Azri Abdul Aziz and Associate Professor Dr. Mohd Nizam Lani (UMT) for offering me advice, listening, and supporting me through this entire PhD journey. Besides that, I would like to thank Mr. Hairul Lail Ismail from Advance Precision Laboratory. He helps me a lot in prototype fabrication for exhibition competitions.

ABSTRACT

Nowadays, thermal management becomes one of the major bottlenecks that restrict the further development of compact electronic devices. This restriction is because of the unpredicted increment of power density in the high-density microchip, which generates high heat flux. To reduce the excessive heat, the CPU throttling technology will slow down the performance of electronic devices by reducing the frequency of microchips. Thus, to ensure electronic devices always perform at their optimum condition, a cooling system with an advanced cooling technique, such as microchannel heat sink (MCHS), is needed to ensure the operating temperature of electronic devices does not exceed the allowable temperature of the semiconductor components. However, conventional MCHS is inadequate to remove the heat flux effectively due to the thermal resistance in the laminar region and pumping power issue. In the present study, the hydrothermal performance of hybrid MCHS designed with the rib-cavity structure was optimised via secondary channel geometry parameters numerically and validated experimentally under laminar flow conditions. Firstly, the numerical approach was initially verified through the validation of the conventional MCHS. Secondly, a comparative study was conducted between the hybrid MCHS with other related enhanced MCHSs, namely, rectangular-rib MCHS, triangular-cavity MCHS, and rib-cavity MCHS. Thirdly, the hydrothermal optimisation of the hybrid MCHS was performed via parametric optimisation of secondary channel angles, secondary channel locations at the cavity structure, and secondary channel widths. Finally, the numerical result was validated experimentally based on the measurement of the Nusselt number and friction factor parameters. The results showed that the secondary channel geometries in the rib-cavity structure of the hybrid MCHS increased the heat transfer performance by 2.1% with the reduction of pumping power consumption by 82.2%. After the parametric optimisation of secondary channel geometry, the hybrid MCHS achieved a performance factor higher than 2.0 at the Reynold number of 450. The performance factor of the optimised hybrid MCHS was 2.02 at the Reynolds number of 450. The highest performance factor achieved by the optimised hybrid MCHS was 2.10 at the Reynolds number of 600 with the minimal entropy generation number of 0.58. The simulation result of the Nusselt number and friction factor showed a good agreement with the experiment, which was less than 20%. With this optimised hybrid MCHS as a cooling device, it can improve the heat transfer performance by 41.3% with a reduction of pumping power consumption by 83.7%. In addition, the coolant consumption has been saved up to 68.9%. Thus, this hybrid MCHS is suitable for a compact electronic device that does not require high energy and coolant consumption for its cooling system. This hybrid MCHS is potentially explored for the usage of other electronic devices and applications. Several interesting aspects may be explored further by investigating the combination of secondary channel geometry with the various shapes of cavity geometry in hybrid MCHS as it affects the recirculation flow formation. Besides that, the utilisation of nanofluid in the hybrid MCHS should be considered together with the concave dimple geometry as the geometry can reduce the surface friction between the nanofluid and channel wall.

ABSTRAK

Kini, pengurusan haba menjadi salah satu halangan utama yang menyekat perkembangan pembangunan peranti elektronik yang padat. Ia berpunca daripada peningkatan ketumpatan kuasa tidak terjangka dalam mikrocip berkepadatan tinggi, di mana ia menghasilkan fluks haba yang tinggi. Untuk mengurangkan haba berlebihan itu, teknologi pendikit CPU akan memperlahankan prestasi peranti elektronik melalui pengurangan frekuensi mikrocip. Oleh itu, untuk memastikan peranti elektronik berfungsi pada tahap optimum, sistem penyejukan yang menggunakan teknik penyejukan termaju, seperti sinki haba saluran mikro (MCHS), diperlukan bagi memastikan suhu peranti elektronik tidak melebihi suhu yang dihadkan untuk komponen semikonduktor. Namun begitu, MCHS konvensional tidak mampu menyingkirkan fluks haba secara efektif kerana masalah rintangan terma dalam aliran laminar, dan masalah kuasa mengepam. Dalam kajian ini, prestasi hidroterma MCHS hibrid yang direka bentuk dengan struktur rusuk-rongga telah dioptimumkan melalui parameter geometri saluran sekunder secara berangka dan telah disahkan secara eksperimen dalam keadaan aliran laminar. Pertama, pendekatan berangka pada mulanya telah disahkan melalui pengesahan MCHS konvensional. Kedua, kajian perbandingan telah dilakukan di antara MCHS hibrid tersebut dengan MCHS yang berkaitan seperti MCHS dengan rusuk-segi-empat-tepat, MCHS dengan rongga-segi-tiga, dan MCHS dengan rusuk-rongga. Ketiga, pengoptimuman hidroterma MCHS hibrid telah dilakukan melalui pengoptimuman parametrik sudut saluran sekunder, lokasi saluran sekunder di struktur rongga, dan lebar saluran sekunder. Akhirnya, hasil kajian berangka telah disahkan secara eksperimen berdasarkan pengukuran parameter nombor Nusselt dan faktor geseran. Hasil kajian telah menunjukkan bahawa geometri saluran sekunder di dalam struktur rusuk-rongga MCHS hibrid telah meningkatkan prestasi pemindahan haba sebanyak 2.1% dengan pengurangan penggunaan kuasa pengepaman sebanyak 82.2%. Selepas pengoptimuman parametrik geometri saluran sekunder, MCHS hibrid tersebut telah mencapai faktor prestasi lebih daripada 2.0 pada nombor Reynolds, 450. Faktor prestasi MCHS hibrid yang telah dioptimumkan pada nombor Reynolds, 450 adalah 2.02. Faktor prestasi tertinggi yang telah dicapai oleh MCHS hibrid yang dioptimumkan ialah 2.10 pada nombor Reynolds, 600 dengan nombor penjanaan entropi minimum, 0.58. Hasil kajian simulasi untuk nombor Nusselt dan faktor geseran telah menunjukkan persetujuan yang baik dengan eksperimen, iaitu kurang daripada 20%. Dengan MCHS hibrid yang dioptimumkan ini sebagai peranti penyejuk, ia boleh meningkatkan prestasi pemindahan haba sebanyak 41.3% dengan pengurangan penggunaan kuasa pengepaman sebanyak 83.7%. Di samping itu, penggunaan bahan pendingin dijimatkan sehingga 68.9%. Oleh itu, MCHS hibrid ini sesuai untuk peranti elektronik yang padat dan tidak memerlukan penggunaan tenaga dan bahan pendingin yang tinggi untuk sistem penyejukannya. MCHS hibrid ini juga berpotensi untuk dikaji bagi kegunaan peranti elektronik dan aplikasi yang lain. Beberapa aspek menarik boleh diterokai dengan lebih lanjut melalui kajian gabungan geometri saluran sekunder dengan pelbagai bentuk geometri rongga dalam MCHS hibrid kerana ia mempengaruhi pembentukan aliran peredaran semula. Selain itu, penggunaan bendalir nano dalam MCHS hibrid perlu dipertimbangkan bersama-sama dengan geometri lesung cekung kerana geometri tersebut boleh mengurangkan geseran permukaan antara bendalir nano dan dinding saluran.

TABLE OF CONTENTS

	TITLE	PAGE
	DECLARATION	iii
	DEDICATION	iv
	ACKNOWLEDGEMENT	v
	ABSTRACT	vi
	ABSTRAK	vii
	TABLE OF CONTENTS	viii
	LIST OF TABLES	xii
	LIST OF FIGURES	xiv
	LIST OF ABBREVIATIONS	xix
	LIST OF SYMBOLS	xx
	LIST OF APPENDICES	xxv
CHAPTER 1	INTRODUCTION	1
1.1	Background of Study	1
1.2	Problem Statement	5
1.3	Research Objectives	7
1.4	Research Scopes	8
1.5	Contributions	9
1.6	Thesis Outline	10
CHAPTER 2	LITERATURE REVIEW	13
2.1	Introduction	13
2.2	Hydrothermal Performance Enhancement Technique	13
2.2.1	Active Method	14
2.2.2	Passive Method	15
2.2.2.1	MCHS with Single Passive Method	15
2.2.2.2	MCHS with Hybrid Passive Method	19

	2.2.2.3	The Utilisation of Nanofluid in a MCHS with Passive Design	33
	2.2.2.4	Optimum Overall Performance of Hybrid MCHS	45
	2.2.2.5	Experimental Study of Hybrid MCHS	48
2.3		Summary	50
CHAPTER 3		RESEARCH METHODOLOGY	55
3.1		Introduction	55
3.2		Research Framework	55
3.3		Analysis Approach	59
	3.3.1	Numerical Simulation Approach	59
	3.3.1.1	Geometry Parameters of MCHSs	60
	3.3.1.2	Governing Equation	62
	3.3.1.3	Boundary Condition	64
	3.3.1.4	Grid Independence Test (GIT)	66
	3.3.1.5	Data Acquisition	73
	3.3.1.6	Overall Performance Evaluation	74
	3.3.1.7	Simulation Model Verification via CR MCHS Validation	77
	3.3.2	Experimental Approach	78
	3.3.2.1	Test Rig	79
	3.3.2.2	Apparatus Specification	81
	3.3.2.3	Experimental Procedures	82
	3.3.2.4	Data Reduction	86
	3.3.2.5	Preliminary Study	92
	3.3.2.6	Uncertainties Analysis	95
3.4		Summary	97
CHAPTER 4		RESULTS AND DISCUSSION	99
4.1		Introduction	99
4.2		Numerical Analysis	99

4.2.1	The Verification of Numerical Model Approach through the CR MCHS Validation	99
4.2.2	Fluid Flow and Heat Transfer Characteristics of CR MCHS	102
4.2.3	Fluid Flow Characteristics in the Enhanced MCHS	105
4.2.3.1	Velocity Distribution	106
4.2.3.2	Pressure Distribution	110
4.2.4	Heat Transfer Characteristics in the Enhanced MCHS	115
4.2.5	Overall Performance of the Enhanced MCHSs	127
4.2.5.1	Performance Factor, PF	127
4.2.5.2	Augmentation Entropy Generation Number, $N_{s,a}$	131
4.2.6	Hydrothermal Optimisation of the TC-RR-SC MCHS via SC Geometry Parameters	135
4.2.6.1	The Effect of SC Angle on the Hydrothermal Performance	136
4.2.6.2	The Effect of SC Location on the Hydrothermal Performance	146
4.2.6.3	The Effect of SC Width on the Hydrothermal Performance	157
4.2.7	Sustainable Cooling Solution in Optimized TC-RR-SC MCHS Versus CR MCHS	168
4.3	Experimental Analysis	171
4.3.1	Formulation of the Regression Equations of Hydrothermal Performance	172
4.3.2	Validation of TC-RR-SC MCHS Simulation Model	174
4.4	Summary	177
CHAPTER 5	CONCLUSIONS AND RECOMMENDATIONS	179
5.1	Conclusions	179
5.2	Recommendations for Future Works	180
REFERENCES		183

LIST OF TABLES

TABLE NO.	TITLE	PAGE
Table 2.1	Advanced structures, challenges and limitations of passive methods in a microchannel	24
Table 2.2	Utilisation of nanofluids in the MCHS application with different nanoparticle concentration/diameter and flow condition	36
Table 3.1	SC geometry parameters for hydrothermal performance optimisation	58
Table 3.2	Geometry parameters of MCHSs	62
Table 3.3	Hydrothermal boundary condition	65
Table 3.4	The GIT analysis and mesh quality of CR MCHS	68
Table 3.5	The GIT analysis and mesh quality of CR-RR MCHS	69
Table 3.6	The GIT analysis and mesh quality of TC MCHS	70
Table 3.7	The GIT analysis and mesh quality of TC-RR MCHS	71
Table 3.8	The GIT analysis and mesh quality of TC-RR-SC MCHS	72
Table 3.9	Apparatus specification	81
Table 3.10	Equipment limit test conditions	94
Table 3.11	The uncertainties of the measurable parameters in experiment	97
Table 4.1	Relative error of the simulation model approach	100
Table 4.2	Convective heat transfer area of the studied MCHSs	118
Table 4.3	Pumping power, P_p and mass flow rate, \dot{m} required by the enhanced MCHSs to achieve the lowest average temperature of bottom surface, $T_{b,ave}$ of CR MCHS	124
Table 4.4	The average temperature of the bottom surface, $T_{b,ave}$ (K) of the studied MCHSs at identical conditions	125
Table 4.5	Pumping power, P_p and mass flow rate, \dot{m} required by the optimised TC-RR-SC MCHS to achieve the lowest overall thermal resistance, R_T of CR MCHS	170

Table 4.6	The overall thermal resistance, R_T of the optimised TC-RR-SC MCHS and CR MCHS at identical condition	170
-----------	---	-----

LIST OF FIGURES

FIGURE NO.	TITLE	PAGE
Figure 1.1	Evolution of transistor count according to Moore's law [12]	2
Figure 1.2	Evolution of microchip size [14, 15]	2
Figure 2.1	Enhancement techniques for MCHS [106]	14
Figure 2.2	Hybrid MCHS with secondary channel geometry [128]	33
Figure 2.3	Type of base fluids commonly used in nanofluid preparation [106]	43
Figure 2.4	Type of nanoparticles commonly used in nanofluid preparation [106]	44
Figure 2.5	Distribution of nanoparticle concentration commonly used in MCHS applications [106]	44
Figure 3.1	Flowchart of the research framework	56
Figure 3.2	Burrs around the top of the fabricated hybrid MCHS	59
Figure 3.3	Debris at the top and bottom of the microchannel	59
Figure 3.4	Single-wall-symmetrical-channel MCHS	60
Figure 3.5	Computational domain of (a) CR MCHS (b) CR-RR MCHS (c) TC MCHS (d) TC-RR MCHS (e) TC-RR-SC MCHS	61
Figure 3.6	Structured mesh with uniform hexahedron and quadrilateral shape for (a) CR MCHS (b) CR-RR MCHS (c) TC MCHS (d) TC-RR MCHS (e) TC-RR-SC MCHS	67
Figure 3.7	The test rig of the optimised TC-RR-SC MCHS (a) Test rig design (b) Exploded view of test rig	79
Figure 3.8	Manifold with aluminium block (a) Isometric view (b) A-A cross-section	80
Figure 3.9	Aluminium block (a) Isometric view (b) Dimensional drawing	80
Figure 3.10	Schematic diagram of the experimental setup	82
Figure 3.11	Experiment apparatus with adjustable table	83
Figure 3.12	Front view of TC-RR-SC MCHS device	84
Figure 3.13	Fluid flow process setup	84

Figure 3.14	Pressure transducer reading for the stable flow rate condition	85
Figure 3.15	Temperature reading for the steady-state condition	85
Figure 3.16	Flow chart of the average Nusselt number calculation	86
Figure 3.17	The locations of three thermocouples in the upper body of the aluminium block (All dimensions in mm)	89
Figure 3.18	Flow trajectory through different regions of the manifold and the fabricated MCHS	92
Figure 3.19	Tube selection for the fluid transportation: (a) Silicon tube, and (b) Pumpsil tube	93
Figure 3.20	Peristaltic pump (a) with pumpsil tube, (b) without pumpsil tube	94
Figure 3.21	Effect of high volume flow rate (<50 ml/min): (a) Overload reading on pressure transducer, (b) Blown pump fuse, (c) Burst pumpsil tube	95
Figure 4.1	Numerical model validation of CR MCHS (a) Local Nusselt number, (b) Pressure drop (Pa), (c) Average friction factor, (d) Temperature difference between the inlet and outlet of channels (K)	102
Figure 4.2	Local Nusselt number at the channel length of CR MCHS	103
Figure 4.3	Temperature distribution (K) in CR MCHS on the x-y plane ($z = 0.25 \text{ mm}$) at (a) $Re = 100$ (b) $Re = 500$ (c) $Re = 800$	104
Figure 4.4	Pressure distribution (Pa) in CR MCHS on the x-y plane ($z = 0.25 \text{ mm}$) at (a) $Re = 100$ (b) $Re = 500$ (c) $Re = 800$	104
Figure 4.5	Velocity contour and streamline distributions (m/s) in the studied MCHSs on the x-y plane ($z = 0.25 \text{ mm}$) at (a) $Re=200$, (b) $Re=450$	107
Figure 4.6	Velocity distribution (m/s) and the formation of secondary flows at $Re = 200$ in (a) CR-RR MCHS, (b) TC-RR MCHS, and (c) TC-RR-SC MCHS	109
Figure 4.7	Pressure distribution (Pa) in the studied MCHSs on the x-y plane ($z = 0.25 \text{ mm}$) at $Re=450$	111
Figure 4.8	Pressure distribution (Pa) on the y-z plane ($x = 6.67 \text{ mm}$) at $Re=450$ for: (a) CR-RR MCHS, (b) TC-RR MCHS, and (c) TC-RR-SC MCHS	113
Figure 4.9	The pumping power (mW) consumption of the studied MCHSs	115

Figure 4.10	Temperature distribution (K) in the studied MCHSs on the x-y plane ($z = 0.25\text{ mm}$) at $Re=450$	117
Figure 4.11	Average wall temperature, $T_{w,ave}$ (K) of the studied MCHSs	118
Figure 4.12	Temperature distribution (K) at the sidewalls of (a) CR MCHS, (b) TC MCHS, (c) CR-RR MCHS, (d) TC-RR MCHS, and (e) TC-RR-SC MCHS at $Re=450$	121
Figure 4.13	The average temperature of the bottom surface, $T_{b,ave}$ (K) of the studied MCHSs and the pumping power, P_p (mW) consumption	123
Figure 4.14	Overall thermal resistance (K/W) in the studied MCHSs	126
Figure 4.15	Friction factor ratio of the enhanced MCHSs	128
Figure 4.16	Nusselt number ratio of the enhanced MCHSs	129
Figure 4.17	Performance factor of the enhanced MCHSs	130
Figure 4.18	Entropy generation rate (W/K) of the enhanced MCHSs caused by the friction loss	132
Figure 4.19	Entropy generation rate (W/K) of the enhanced MCHSs caused by the heat transfer process	133
Figure 4.20	The augmentation entropy generation number of the enhanced MCHSs	134
Figure 4.21	The effect of the secondary channel angles of TC-RR-SC MCHS on the friction factor ratio	136
Figure 4.22	Pressure distribution (Pa) in TC-RR-SC MCHS on the x-y plane ($z = 0.25\text{ mm}$) at (a) $Re=200$, (b) $Re=350$ and $Re=550$ for the SC angle of 15° , 30° , 45° and 60°	139
Figure 4.23	The effect of the secondary channel angles of TC-RR-SC MCHS on the Nusselt number ratio	139
Figure 4.24	Temperature distribution (K) in TC-RR-SC MCHS on the x-y plane ($z = 0.25\text{ mm}$) at (a) $Re=200$, (b) $Re=350$, and (c) $Re=550$, for the SC angle of 15° , 30° , 45° and 60°	141
Figure 4.25	The effect of the secondary channel angle of TC-RR-SC MCHS on performance factor	142
Figure 4.26	The effect of the secondary channel angle of TC-RR-SC MCHS on the entropy generation rate caused by the friction lost	144

Figure 4.27	The effect of the secondary channel angle of TC-RR-SC MCHS on the entropy generation rate caused by the heat transfer process	144
Figure 4.28	The effect of the secondary channel angle of TC-RR-SC MCHS on the augmentation entropy generation number	145
Figure 4.29	The improvement of PF of TC-RR-SC MCHS after optimisation process	146
Figure 4.30	The effect of the secondary channel location of TC-RR-SC MCHS on the friction factor ratio	148
Figure 4.31	Pressure distribution (Pa) in TC-RR-SC MCHS on the x-y plane ($z = 0.25\text{ mm}$) at (a) $Re=200$, (b) $Re=350$, and (c) $Re=550$, for the SC location of $10\ \mu\text{m}$, $25\ \mu\text{m}$ and $40\ \mu\text{m}$	150
Figure 4.32	The effect of the secondary channel location of TC-RR-SC MCHS on the Nusselt number ratio	150
Figure 4.33	Temperature distribution (K) in TC-RR-SC MCHS on the x-y plane ($z = 0.25\text{ mm}$) at (a) $Re=200$, (b) $Re=350$, and (c) $Re=550$, for the SC location of $10\ \mu\text{m}$, $25\ \mu\text{m}$ and $40\ \mu\text{m}$	152
Figure 4.34	The effect of the secondary channel location of TC-RR-SC MCHS on performance factor	153
Figure 4.35	The effect of the secondary channel location of TC-RR-SC MCHS on the entropy generation rate caused by the friction lost	155
Figure 4.36	The effect of the secondary channel location of TC-RR-SC MCHS on the entropy generation rate caused by the heat transfer process	155
Figure 4.37	The effect of the secondary channel location of TC-RR-SC MCHS on the augmentation entropy generation number	157
Figure 4.38	The effect of the secondary channel width of TC-RR-SC MCHS on the friction factor ratio	158
Figure 4.39	Pressure distribution (Pa) in TC-RR-SC MCHS on the x-y plane ($z = 0.25\text{ mm}$) at (a) $Re=200$, (b) $Re=350$, and (c) $Re=550$, for the SC width of $20\ \mu\text{m}$, $30\ \mu\text{m}$, $40\ \mu\text{m}$ and $50\ \mu\text{m}$	160
Figure 4.40	The effect of the secondary channel width of TC-RR-SC MCHS on the Nusselt number ratio	161
Figure 4.41	Temperature distribution (K) in TC-RR-SC MCHS on the x-y plane ($z = 0.25\text{ mm}$) at (a) $Re=200$, (b) $Re=350$, and (c) $Re=550$, for the SC width of $20\ \mu\text{m}$, $30\ \mu\text{m}$, $40\ \mu\text{m}$, and $50\ \mu\text{m}$	163

Figure 4.42	The effect of the secondary channel width of TC-RR-SC MCHS on performance factor	164
Figure 4.43	The effect of the secondary channel width of TC-RR-SC MCHS on the entropy generation rate caused by the friction lost	165
Figure 4.44	The effect of the secondary channel width of TC-RR-SC MCHS on the entropy generation rate caused by the heat transfer process	166
Figure 4.45	The effect of the secondary channel width of TC-RR-SC MCHS on the augmentation entropy generation number	167
Figure 4.46	Performance factor of all optimum SC geometry parameters	168
Figure 4.47	The overall thermal resistance, $R_T (K/W)$, and pumping power, P_p of the optimised TC-RR-SC MCHS and CR MCHS	169
Figure 4.48	The average temperature of the bottom surface, $T_{b.ave} (K)$, of CR MCHS and TC-RR-SC MCHS	171
Figure 4.49	Experimental result of the Nusselt number, Nu_{ave} of optimised TC-RR-SC MCHS	173
Figure 4.50	Experimental result of the friction factor, f_{app} of optimised TC-RR-SC MCHS	174
Figure 4.51	Validation of the numerical result of Nusselt number, Nu_{ave} with experimental result	175
Figure 4.52	Validation of the numerical result of friction factor, f_{app} with experimental result	176

LIST OF ABBREVIATIONS

CAGR	-	Compound annual growth rate
CFD	-	Computational Fluid Dynamics
COVID-19	-	Coronavirus Disease 2019
CR MCHS	-	Conventional-Rectangular Microchannel Heat Sink
CR-RR MCHS	-	Rectangular-Rib Microchannel Heat Sink
DI	-	Deionised
EG	-	Ethylene Glycol
EMF		Electromotive Force
GIT	-	Grid Independence Test
HT	-	Heat Transfer
Kn	-	Knudsen Number
MCHS	-	Microchannel Heat Sink
MOEA	-	Multi-objective Evolutionary Algorithm
MTTF	-	Mean Time to Failure
MWCNT	-	Multi-Walled Carbon Nanotube
MyIPO	-	Intellectual Property Corporation of Malaysia
PF	-	Performance Factor
Po	-	Poiseuille Number
POM	-	Polyoxymethylene
Pr	-	Prandtl Number
Re	-	Reynolds number
SC	-	Secondary Channel
SWCNT	-	Single-Wall Carbon Nanotube
TC MCHS	-	Triangular-Cavity Microchannel Heat Sink
TC-RR MCHS	-	Triangular-Cavity-Rectangular-Rib Microchannel Heat Sink
TC-RR-SC MCHS	-	Triangular-Cavity-Rectangular-Rib-Secondary- Channel Microchannel Heat Sink

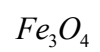
LIST OF SYMBOLS

ε / D	-	Effective Roughness Ratio
Ω	-	Fluid Domain
η	-	The Coefficient of Area
ρ_f	-	Density of Fluid
μ_f	-	Dynamic Viscosity of Fluid
α_c	-	Aspect Ratio (Width/Height) of CR MCHS
c_{pf}	-	Heat Capacity of Fluid
k_f	-	Thermal Conductivity of Fluid
k_{al}	-	Thermal Conductivity of Aluminium
Nu_{ave}	-	Nusselt number
Nu_x	-	Local Nusselt Number
(Nu/Nu_o)	-	Nusselt Number Ratio
Nu_o	-	Nusselt Number in the CR MCHS
$N_{s,a}$	-	Augmentation Entropy Generation Number
f_{app}	-	Apparent friction factor
(f/f_o)	-	Friction Factor Ratio
f_o	-	Friction Factor in the CR MCHS
P	-	Pressure
ΔP	-	Pressure Drop
ΔP_{tot}	-	Total Pressure Loss
ΔP_{mchs}	-	Pressure Loss in the Fabricated MCHS
ΔP_{sc}	-	Pressure Loss due to Sudden Contraction
ΔP_{se}	-	Pressure Loss due to Sudden Expansion
ΔP_{dis}	-	Display Value of Pressure Transducer
ΔP_{cal}	-	Calibrated Pressure Drop

P_p	-	Pumping Power Consumption
P_w	-	Wall Perimeter
R_T	-	Thermal Resistance
$(COP)_r$	-	Coefficient of Performance Ratio
ΔT_{ave}	-	Average Temperature Difference
$T_{b,ave}$	-	The Average Temperature at the Bottom Wall of MCHS
T_f	-	Temperature of Fluid
T_{bulk}	-	Bulk Temperature of Fluid
T_w	-	Wall Temperature
$T_{w,ave}$	-	Average Temperature of Microchannel Wall
T_{max}	-	Maximum Temperature
T_{min}	-	Minimum Temperature
T_{in}	-	Inlet Temperature
T_{out}	-	Outlet Temperature
T_{wb}	-	Water Bath Temperature
T_{emf}	-	Thermocouple Temperature Converted from Thermocouple Voltage
T_1	-	Inlet Temperature of the Fabricated MCHS
T_2	-	The Temperature of the Fabricated MCHS Close to its Inlet Area
T_3	-	The Temperature of the Fabricated MCHS Close to its Outlet Area
T_4	-	Outlet Temperature of the Fabricated MCHS
T_5	-	The Temperature of the Fabricated MCHS at its centre
h_{ave}	-	Average Heat Transfer Coefficient
q_w	-	The Applied Heat Flux
Q_{sen}	-	Sensible Heat
u	-	Velocity Component in X-Direction

v	-	Velocity Component in Y-Direction
w	-	Velocity Component in Z-Direction
u_m	-	Mean Velocity
U	-	The Velocity of the Distilled Water
V	-	Fluid Volume
\dot{V}	-	Volume Flow Rate
\dot{m}	-	Mass Flow Rate
A_{film}	-	The Heated Area
$A_{conv.}$	-	Convective Heat Transfer Area
A_c	-	The Cross-Section Area of the Channel Wall
A_{in}	-	Channel Inlet Cross-Section Area
A_t	-	The Total Area of Convective Heat Transfer
A_{bc}	-	The Unfinned Area at the Bottom Surface of Microchannels
A_{fin}	-	The Area of Fin
A_{ubb}	-	The Base Area of the Aluminium Block Upper Body
D_h	-	Hydraulic Diameter
$\frac{e_1}{D_h}$	-	Relative Re-entrant Cavity Height
$\frac{e_2}{D_h}$	-	Relative Rib Height
A_{sc}	-	Secondary Channel Angle
L_{sc}	-	Secondary Channel Location at Cavity Structure
W_{sc}	-	Secondary Channel Width
L_t	-	Total Length of Microchannel
W_t	-	Total Width of Single-Wall-Symmetrical-Channel MCHS
H_t	-	Total Height of MCHS
H_c	-	Height of Microchannel
W_c	-	Width of Microchannel
L_r	-	Length of Rib Geometry

W_r	-	Width of Rib Geometry
La	-	Length between the Leading Edge of Rib Geometries
$L1$	-	Horizontal Length of the Shortest Edge of Cavity Geometry
$L2$	-	Horizontal Length of the Longest Edge of Cavity Geometry
$L3$	-	Length between Two Adjacent Cavity Geometries
W_{tc}	-	Distance between the corner of two opposite cavity geometries
W_w	-	The Thickness of The Channel Wall
S	-	The Distance Between Thermocouple and the Bottom Surface of Microchannel
$\dot{S}_{gen,\Delta T}$	-	Entropy Generation Rate Caused by the Heat Transfer
$\dot{S}_{gen,\Delta p}$	-	Entropy Generation Rate Caused by the Friction Loss
\dot{S}_{gen}	-	The Total Entropy Generation Rate
$\dot{S}_{gen,o}$	-	Total Entropy Generation Rate in the CR MCHS
K	-	Hagenbach's Factor
K_e	-	The Loss Coefficient of Sudden Expansion
K_c	-	The Loss Coefficient of Sudden Contraction
v/v	-	Volume Fraction
w/v	-	Weight Fraction
Al_2O_3	-	Aluminium oxide
SiO_2	-	Silicon Dioxide
TiO_2	-	Titanium Dioxide
Cu	-	Copper
CuO	-	Copper Oxide
Zn	-	Zinc
SiC	-	Silicon Carbide
Ag	-	Silver



- Iron (II, III) Oxide

LIST OF APPENDICES

APPENDIX	TITLE	PAGE
Appendix A	Test rig	201
Appendix B	Optimised hybrid MCHS parameter	211
Appendix C	Calibration	212
Appendix D	The supplied heat flux measurement	216
Appendix E	Uncertainty	217
Appendix F	Test rig table	221
Appendix G	Correlation analysis	222
Appendix H	Regression analysis	225

CHAPTER 1

INTRODUCTION

1.1 Background of Study

Application of cooling system in thermal engineering is recognised and have been studied both theoretically and practically in building energy system, electronic devices, chemical vapour deposition instruments, solar energy collectors, furnace engineering and many more [1]. In recent years, thermal management of electronic devices is of interest as a new generation of high performing dense chip packages that function at high frequency produces a high heat flux on the electronic devices. Prolonged heat flux creates a hot spot on the electronic devices and reduces the lifespan of the electronic devices [2, 3] due to the acceleration of the Mean Time to Failure (MTTF) as described by the Black's equation [4]. Thermal management of compact electronic devices that operate at high power density is critical as there is a lack of efficient technique to remove heat dissipation from the electronic devices [5-8].

According to Moore's law used by Intel for transistor count observation, it demonstrates that the number of transistors doubling every 24 months [9-13] as shown in Figure 1.1 [10]. There are three measures considered in the increasing number of transistors per microchips, such as shrinking the size of the single transistor (scaling), increasing the microchip area, and improving circuit and device design. As seen in Figure 1.2, scaling down the individual transistor and microchip size in improving the microprocessor performance [14, 15] has caused detrimental effects that leading to high heat dissipation. That is one of the biggest challenges in microchip development [16]. As a consequence, urgent needs for the advanced cooling device is raising by years. Based on the Market Research Report [17], microchannel cooling is one of the cooling technology that expected to grow at the highest Compound Annual Growth Rate (CAGR) in the global thermal management market for the global forecast of the year 2025.

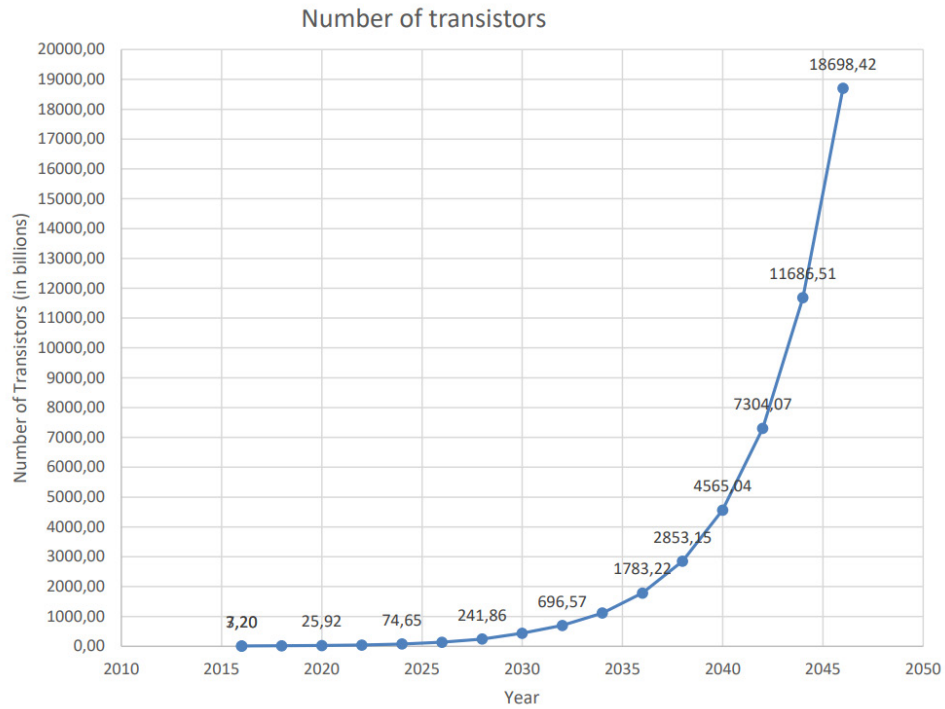


Figure 1.1 Evolution of transistor count according to Moore's law [12]

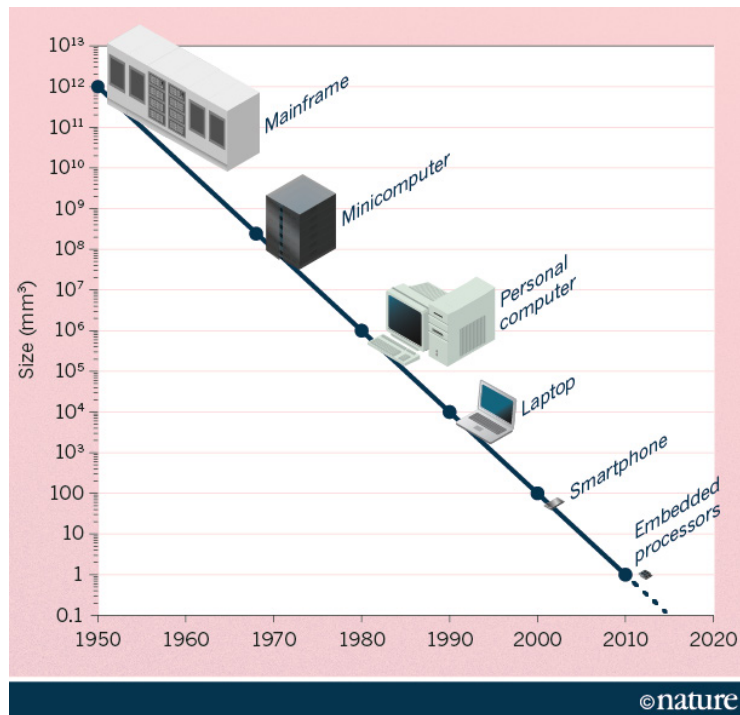


Figure 1.2 Evolution of microchip size [14, 15]

The increase in power density and miniaturisation of electronic packages has changed the direction of cooling system technology, from air-cooling technology to

the advanced heat transfer technology due to the inadequacy of conventional method to remove extreme high heat flux [18].

Several methods have been proposed in the previous studies to improve the cooling performance, such as air cooling method [19], heat pipe method [20], use of liquid material as a coolant [21], and micro-cooling method [22-24]. Micro-cooling is a good technique due to its high cooling efficiency compared to the other methods. Even though the air cooling method is the simplest cooling technique, it has a low cooling efficiency with additional heat generation by the fan itself [25]. Meanwhile, for the liquid material and heat pipe applications, space is required to accommodate additional system for condensation process [25] which are not suitable for compact electronic devices. Therefore, the micro-cooling method is one of the most promising techniques that can dissipate a high heat flux generated by the compact electronic devices that can be attributed to the high heat transfer surface-area-to-volume ratio. Besides that, the micro hydraulic diameter also contributes to the heat transfer performance enhancement due to the augmentation of heat transfer coefficient [26].

When the micro-cooling method is used, microchannel heat sink (MCHS) is found to be the most prospective as a high heat flux can be removed compared to micro-jet impingement, micro-heat pipe and micro-electro-hydrodynamic methods [27]. In 1981, Tuckerman and Pease [28] reported that rectangular MCHS can remove heat-flux up to 790 W/cm^2 . However, the pumping power required by the MCHS was high due to high-pressure drop penalty generated in the microchannel. Based on the study of Japar et al. [29], high-pressure drop penalty attributed to the high wall shear stress in the developing region of laminar flow. This important discovery motivates many scholars to investigate the performance of rectangular microchannel via geometry parameters and stacked layer optimisations.

In the geometry parameter optimisation of rectangular MCHS, the thermal and hydraulic resistances decreased with increasing aspect ratio of a rectangular microchannel (channel width to channel height) [30]. This is because MCHS with high aspect ratio provide a larger convective heat transfer area and flow cross-section area. The findings were further supported by Kowsari et al. [31] where for a smaller and

constant cross-section area, the heat transfer performance increased with channel aspect ratio. In-depth effect of a rectangular channel aspect ratio on the thermal performance was investigated by Sobhan et al. [32] and Kou et al. [33]. The authors found that at a fixed aspect ratio, channel width significantly affected thermal resistance as the bottom channel area lied directly under the applied heat flux. Besides the thermal resistance issue, the pressure drop penalty is also an aim of rectangular channel MCHS optimisation process.

One of the related studies includes investigation of hydrothermal performance in a single-layered and double-layered MCHS to reduce the pressure drop penalty by Chong et al. [34]. The study demonstrated that in the laminar region, the double-layered MCHS reduced the pressure drop, ΔP by 53.9% compared to the single-layered MCHS. However, the thermal resistance in the double-layered MCHS was higher than the single-layered MCHS by 20.8%. A solution was proposed by Wei et al. [35] to reduce the thermal resistance in a stacked MCHS, either to increase the pumping power or to reduce the channel length. Hung et al. [36] also recommended increasing the pumping power to mitigate the optimal thermal resistance. However, in another study by Wang et al. [37], both thermal resistance and pumping power consumption were improved simultaneously through optimisation of semi-porous rib geometry. The researchers reported that the double-layered MCHS with the optimised semi-porous-rib geometry improved the cooling performance and pumping power by 14.06% and 16.40%, respectively.

Nevertheless, further geometry optimisation of a rectangular channel MCHS is limited by pressure drop penalty in a mono-layered MCHS and additional space requirement by a multi-layered MCHS in the cooling system of a compact electronic device. In recent years, many investigations have been conducted to further improve the performance of MCHS through advanced geometric structure and nanofluid [38] which can provide high cooling performance with less pumping power consumption. The cooling demand can be achieved by designing a sustainable enhanced MCHS with three criteria: (1) High cooling performance; (2) Low coolant and energy consumptions; (3) Small and compact heat sink [39]. Hybrid MCHS is one of the best

methods which can meet those criteria. Hybrid MCHS is a MCHS that integrated with more than one passive method in its microchannels in order to:

- (a) Increase the convective heat transfer area of microchannel via fin geometry, and cavity or dimple structure.
- (b) Reduce the local pressure drop penalty via cavity or dimple structure. Those structures will enlarge the flow area in microchannel and thus reduce the pumping power consumption.
- (c) Redevelop boundary layer in the laminar region via flow disruptions method so that the thermal resistance can be reduced and thus improve the cooling performance.
- (d) Increase the degree of fluid mixing between hot and cold coolant by promoting the vortices flow formation in microchannels.

Based on the study conducted by Lu et al. [40], it is worth mentioning here that a hybrid MCHS can improve or negatively affect the overall performance of MCHS. For this reason, a comprehensive analysis needs to be conducted further for the hybrid MCHS designs. The combined effect of implemented methods on the fluid flow and heat transfer characteristics in the hybrid MCHS is a key factor that determines the overall performance of the hybrid MCHS. Therefore, this study conducted comprehensive analyses for the development of laminar forced convection cooling in hybrid microchannel heat sink with secondary channel for electronic devices. The findings from this study provides sustainable cooling solutions that can be used in many electronic devices and applications.

1.2 Problem Statement

Demand for high-performance electronic devices has continued to surge as the Fourth Industrial Revolution (IR 4.0) focuses heavily on interconnectivity, automation, machine learning, and real-time data. Thus, high-power integrated circuit

packages (microchips) have been developed further to enhance the performance of electronic devices. As a result, high heat dissipation is generated by electronic devices due to the scaling down effect of tiny transistors on microchips. With the unpredicted increment of power density in microchips, which close to 100 W/cm^2 [41], an advanced cooling technique like MCHS is required to ensure the temperature of electronic devices does not exceed the allowable temperature of the semiconductor component. The allowable temperature is less than 358.15 K [42, 41]). However, the conventional design of conventional-rectangular microchannel heat sink (CR MCHS) is inadequate to effectively remove heat dissipation due to the thickness of the thermal boundary layer in the laminar region and pumping power issue [29]. Besides that, the CR MCHS requires high coolant and pumping power consumptions to reduce the operating temperature to less than the allowable temperature [42].

Hybrid MCHS is an innovative cooling technique that can fulfil the cooling demand for compact electronic devices installed with the advanced microchips. Hybrid MCHS should provide high heat transfer performance with less pumping power consumption. Rib-cavity MCHS is one of the hybrid MCHS than can meet the criteria. However, the recirculation flow in the cavity geometries has deteriorated the heat transfer performance in the cavity geometry as it increases the residence time of fluid to remain longer in the stagnation zone (dead zone) area of cavity geometry [43-47]. Consequently, the heat from the sidewalls of cavity geometry cannot be removed efficiently. Secondary channel (SC) geometry is channels that connect each cavity geometry to the cavity geometry of the adjacent channel. The combination of rib-cavity structure with SC geometries in hybrid MCHS could minimise the size of recirculation flow formation in the cavity geometry area and thus improve the overall heat transfer performance.

Besides that, most of the rib-cavity MCHSs obtained performance factor (PF) lower than 2.0 at the Re of 450 [43, 45-55]. It indicates that those rib-cavity MCHSs required high coolant and pumping power consumptions in order to provide high hydrothermal performance. In addition, most of the rib-cavity MCHSs only considers PF in the design development. However, to implement sustainable cooling solutions in rib-cavity MCHSs, both cooling capacity and energy efficiency should be

considered in the design development. Therefore, the irreversibility (entropy generation rate) associated with the heat transfer process should be analysed together with performance factor, PF in order to determine the overall performance of an innovated MCHS.

The most critical issue in the design development of hybrid MCHS is its fabrication process since most of the design of hybrid MCHSs are too complex. Consequently, it is important to fabricate the proposed hybrid MCHS as there are many limitation during the fabrication process such as the size of cutting tools and micro-machining process. It determines whether the proposed design can be commercialised and transferred to the mass production in electronic industry or not. Besides that, most of researchers still use straight-channel MCHS for their numerical model validation [44, 49, 50, 56-59] because experimental analyses of the fabricated hybrid MCHS such as regression analysis are limited in the previous studies. Regression equation that formulated from the regression analysis can be used as reference for validation purpose in the future study for an innovated MCHS that have similar design with the proposed MCHS.

1.3 Research Objectives

The main goal of this research is to develop a sustainable hybrid MCHS that can provide high heat transfer rate with low coolant and pumping power consumptions. It can be achieved by promoting a high degree of fluid mixing between cold and hot coolant at low Re. In order to achieve these goals, the objectives of this research are formulated as follows:

1. To increase heat transfer performance with less pumping power consumption by integrating secondary channel geometry in the rib-cavity structure of hybrid MCHS that can eliminate the recirculation flow in the cavity geometry.

2. To increase the performance factor of hybrid MCHS higher than 2.0 for the Reynolds number of 450 with minimal entropy generation number by optimising the secondary channel geometry parameters.
3. To validate the numerical model of the optimised design of hybrid MCHS experimentally based on the measurement of Nusselt number and friction factor of the fabricated hybrid MCHS

1.4 Research Scopes

In order to achieve the objectives of the present study, the following scopes are defined. Generally, there are two themes in this study, namely, numerical and experimental analysis of the enhanced MCHS adopted with the hybrid technique of passive method.

1. Hydrothermal performance enhancement techniques in the studied MCHSs were developed by a passive method.
2. Numerical investigations of the studied MCHSs were conducted by single-wall microchannel analysis.
3. Numerical investigations focused on laminar forced convection cooling in the enhanced MCHSs for the Reynolds number of 100 to 800.
4. Hydrothermal optimisation focused on secondary channel geometry parameters, namely, secondary channel angle (15° , 30° , 45° , 60°), secondary channel location ($10\ \mu\text{m}$, $25\ \mu\text{m}$, $40\ \mu\text{m}$) at cavity area, and secondary channel width ($20\ \mu\text{m}$, $30\ \mu\text{m}$, $40\ \mu\text{m}$, $50\ \mu\text{m}$).
5. For the validation purpose, the fabricated MCHS is made of aluminium. The hydrothermal performance of the fabricated MCHS was investigated with the volume flow rate of 44 ml/min to 211 ml/min or the Reynolds number of 100 to 500.

6. Regression equations of hydrothermal performance were formulated based on the optimised hybrid MCHS integrated with SC geometries.

1.5 Contributions

Thermal management is one of the biggest technical challenges facing numerous industries, especially microelectronic sector. Rapid growth in the microelectronic industry is increasing thermal load and requiring faster cooling. Hence, there is an urgent need for an advanced cooling technique like TC-RR-SC MCHS (the combination of triangular cavity, rectangular rib and secondary channel geometries in a single channel of MCHS) to meet the cooling demand. The contributions of the present study are:

1. **Test Rig:** The test rig of TC-RR-SC MCHS was fabricated with the slotted MCHS. Thus, the present MCHS can be replaced with other enhanced MCHSs for experimental study in future. This test rig is suitable for the single-phase and two-phase system. This test rig can be used as teaching aids for demonstration and practical lessons.
2. **Further Development of Microchip:** High heat flux generated by the electronic device becomes the bottleneck of further development of microchip. By having this TC-RR-SC MCHS as a cooling device, the advanced technology can be further developed for the development of technologies in line with Industry 4.0.
3. **Cooling System of Compact Electronic Device:** TC-RR-SC MCHS does not require high coolant and energy consumptions. Thus, smaller microfluidic pump and reservoir tank can be used in cooling systems. Therefore, TC-RR-SC MCHS is suitable for compact electronic devices that require less coolant and energy consumptions for their cooling system due to a small and compact cooling compartment area. With the TR-RR-SC MCHS, thermal performance,

energy and coolant consumptions are improved by 41.3%, 83.7%, and 68.9%, respectively, as compared with the optimum performance of CR MCHS.

4. **Knowledge:** By knowing the fluid flow and heat transfer characteristics in the TC-RR-SC MCHS, a similar geometry structure can be implemented in the future design of MCHS. A high degree of fluid mixing at low flow rate is good for a sustainable cooling device. Besides that, the regression equations of the optimised hydrothermal performance of TC-RR-SC MCHS can be used as the reference in the future study.
5. **Application in other industrial sector:** It is optimistic that this cooling technology can be applied in: (1) Nuclear industry for the heat transportation from the nuclear reactor to the steam generator, (2) Solar industry for solar collector, and (3) Automotive industry for car radiator.

1.6 Thesis Outline

The present thesis consists of five chapters, including this chapter. In general, there are two themes in this thesis, namely, numerical and experimental analyses of the enhanced MCHS adopted with the hybrid technique of passive method. Most of the works in this thesis are numerical study. The experimental study was conducted for the numerical model validation purpose only.

In **Chapter 1**, a general overview of the current cooling demand of high-performance electronic device is discussed comprehensively. Some micro-cooling techniques are compared to find the best cooling techniques that can provide a sustainable cooling system. MCHS is one of the most advanced cooling techniques that can meet the cooling demand. However, the conventional MCHS only achieve its optimum performance at a high flow rate, which affects the coolant and energy consumptions. This issue is discussed in detail in the problem statement section. Then,

the aim, objectives, and scopes are defined in order to set the direction of the present study.

In **Chapter 2**, a comprehensive review of the MCHS performance is presented in order to identify the flow mechanism that helps in the enhancement of the heat transfer performance. Generally, two hydrothermal performance enhancement methods are highlighted, namely, active and passive methods. Nevertheless, the passive method is discussed critically throughout Chapter 2 compared to the active method. Firstly, MCHS with a single passive method was reviewed to identify the advantages and disadvantages of each technique in the passive method. Then, MCHS with hybrid techniques of passive method was examined to investigate how the combined effect of the hybrid technique can improve the heat transfer performance with an acceptable pressure drop. Secondly, the optimization techniques implemented by the previous researcher were discussed comprehensively. Lastly, the experimental studies related to the enhanced MCHS were reviewed in order to investigate the limitation of the experimental analysis. From this review, the research gap was pointed out.

In **Chapter 3**, the used methodologies to conduct this research are presented. The works can be separated into two parts: numerical study, and; experimental study. In the numerical investigation, comparative studies among the studied MCHSs were conducted in order to investigate the effect of the geometry structures on the fluid flow and heat transfer characteristics in a single-wall microchannel. Besides that, the optimisation of PF and minimisation of $N_{s,a}$ were performed in order to identify the optimum overall performance of the proposed hybrid MCHS. All the studied MCHSs were designed and analysed by CATIA-V5R20 and ANSYS-17.0 software, respectively. Besides that, the contour profiles of the studied MCHSs were examined by Tecplot-360. In the experimental study, the friction factor, f_{app} , and the average Nusselt number, Nu_{ave} , of the fabricated MCHS were measured and compared with the numerical model for the validation purpose.

In **Chapter 4**, for simulation study, the overall performances of all the studied MCHSs were determined by PF. Besides that, the augmentation entropy generation numbers, $N_{s,a}$ of all the MCHSs were calculated to measure the fluid flow and heat transfer irreversibility during the heat transfer process. Furthermore, the thermal resistance, R_T , and average temperature, $T_{b,ave}$, at the bottom surface of MCHS were also calculated as the substrate of MCHS is attached directly to the heat source. The effect of geometry structures on the degree of fluid mixing was further investigated by measuring the average wall temperature, $T_{w,ave}$, of the studied MCHSs. Energy consumption of each studied design was calculated by pumping power consumption, P_p . The effects of geometry structures on the fluid flow and heat transfer characteristics were illustrated in the contour profile too. For the experimental study, only two parameters were measured, f_{app} and Nu_{ave} .

In **Chapter 5**, the main conclusions of the present work are drawn together and presented based on the objective of this study. Besides that, the recommendations for the future study are addressed in this section too.

REFERENCES

- [1] Sidik N. A. C., Muhamad M. N. A. W., Japar W. M. A. A. and Rasid Z. A. An overview of passive techniques for heat transfer augmentation in microchannel heat sink. *Int Commun Heat Mass Transfer*. 2017. 88: 74-83.
- [2] Jafaryar M. and Sheikholeslami M. Intensification of performance of pipe with nanoparticle flow along turbulator with obstacles. *Chemical Engineering and Processing-Process Intensification*. 2021. 165: 108426.
- [3] Yadav D., Chu Y.-M. and Li Z. Examination of the nanofluid convective instability of vertical constant throughflow in a porous medium layer with variable gravity. *Applied Nanoscience*. 2021. 1-14.
- [4] Black J. R. Electromigration—A brief survey and some recent results. *IEEE Trans Electron Devices*. 1969. 16(4): 338-47.
- [5] Farsad E., Abbasi S., Zabihi M. and Sabbaghzadeh J. Numerical simulation of heat transfer in a micro channel heat sinks using nanofluids. *Heat and Mass Transfer*. 2011. 47(4): 479-90.
- [6] Sheikholeslami M., Farshad S. A., Ebrahimpour Z. and Said Z. Recent progress on flat plate solar collectors and photovoltaic systems in the presence of nanofluid: a review. *Journal of Cleaner Production*. 2021. 293: 126119.
- [7] Qin Y. Simulation of MHD impact on nanomaterial irreversibility and convective transportation through a chamber. *Applied Nanoscience*. 2021. 1-14.
- [8] Jiang L., Wang Y., Wang X., Ning F., Wen S., Zhou Y., Chen S., Betts A., Jerrams S. and Zhou F.-L. Electrohydrodynamic printing of a dielectric elastomer actuator and its application in tunable lenses. *Composites Part A: Applied Science and Manufacturing*. 2021. 147: 106461.
- [9] Schwierz F. and Liou J. J. Status and Future Prospects of CMOS Scaling and Moore's Law-A Personal Perspective. *2020 IEEE Latin America Electron Devices Conference (LAEDC)*. February 25, 2020. New York: IEEE. 2020. 1-4.
- [10] Chen Y., Yang C., Kuo C., Chen M., Tung C., Chiou W. and Yu D. Ultra High Density SoIC with Sub-micron Bond Pitch. *2020 IEEE 70th Electronic*

- Components and Technology Conference (ECTC)*. June 3-30, 2020. USA: IEEE. 2020. 576-81.
- [11] Schuermans S. and Leupers R. *Power estimation on electronic system level using linear power models*. Switzerland: Springer. 2019.
- [12] El-Aawar H. and Sous A. Applying the Moore's Law for a Long Time using Multi-Layer Crystal Square on a Chip. *2019 IEEE XVth International Conference on the Perspective Technologies and Methods in MEMS Design (MEMSTECH)*. May 22-26, 2019. New York: IEEE. 2019. 12-6.
- [13] Wu J., Shen Y.-L., Reinhardt K., Szu H. and Dong B. A nanotechnology enhancement to Moore's law. *Applied Computational Intelligence and Soft Computing*. 2013. 2013: 13.
- [14] Waldrop M. M. The chips are down for Moore's law. *Nature News*. 2016. 530(7589): 144.
- [15] Waldrop M. M. More than moore. *Nature*. 2016. 530(7589): 144-8.
- [16] Sun S., Narayana V. K., Miscuglio M., Kimerling L. C., El-Ghazawi T. and Sorger V. J. cLeAR: A Holistic figure-of-Merit for post-and predicting electronic and photonic-based compute-system evolution. *Sci Rep*. 2020. 10(1): 1-9.
- [17] Report M. R. Thermal Management Market worth \$12.8 billion by 2025. *MARKETS AND MARKETS*. 2020. <https://www.marketsandmarkets.com/PressReleases/thermal-management.asp>. 2020.
- [18] Ghani I. A., Sidik N. A. C. and Kamaruzaman N. Hydrothermal performance of microchannel heat sink: The effect of channel design. *Int J Heat Mass Transfer*. 2017. 107: 21-44.
- [19] Dugan J. F. and Anderson S. D. *Electronic device fan mounting system*. US6244953B1. 2001
- [20] Chang Y.-W., Cheng C.-H., Wang J.-C. and Chen S.-L. Heat pipe for cooling of electronic equipment. *Energy Convers Manage*. 2008. 49(11): 3398-404.
- [21] Deng Y. and Liu J. A liquid metal cooling system for the thermal management of high power LEDs. *Int Commun Heat Mass Transfer*. 2010. 37(7): 788-91.
- [22] Gong L., Zhao J. and Huang S. Numerical study on layout of micro-channel heat sink for thermal management of electronic devices. *Appl Therm Eng*. 2015. 88: 480-90.

- [23] Alihosseini Y., Targhi M. Z. and Heyhat M. M. Thermo-hydraulic performance of wavy microchannel heat sink with oblique grooved finned. *Appl Therm Eng.* 2021. 189: 116719.
- [24] Zhu Q., Su R., Hu L., Chen J., Zeng J., Zhang H., Sun H., Zhang S. and Fu D. Heat transfer enhancement for microchannel heat sink by strengthening fluids mixing with backward right-angled trapezoidal grooves in channel sidewalls. *Int Commun Heat Mass Transfer.* 2022. 135: 106106.
- [25] Lee J.-h. *Micro cooling device.* US6698502B1. 2004
- [26] Steinke M. E. and Kandlikar S. G. Single-Phase Heat Transfer Enhancement Techniques in Microchannel and Minichannel Flows. *ASME 2004 2nd International Conference on Microchannels and Minichannels.* June 17-19, 2004. New York: ASME. 2008. 141-8.
- [27] Noh N., Fazeli A. and Sidik N. C. Numerical simulation of nanofluids for cooling efficiency in microchannel heat sink. *J Adv Res Fluid Mech Therm Sci.* 2014. 4(1): 13-23.
- [28] Tuckerman D. B. and Pease R. F. W. High-performance heat sinking for VLSI. *IEEE Electron device letters.* 1981. 2(5): 126-9.
- [29] Japar W. M. A. A., Sidik N. A. C., Kamaruzaman N., Asako Y. and Muhammad N. M. a. Hydrothermal performance in the Hydrodynamic Entrance Region of Rectangular Microchannel Heat Sink. *Journal of Advanced Research in Numerical Heat Transfer.* 2020. 1(1): 22-31.
- [30] Khan W. A., Yovanovich M. and Culham J. Optimization of microchannel heat sinks using entropy generation minimization method. *Twenty-Second Annual IEEE Semiconductor Thermal Measurement And Management Symposium.* March 14-16, 2006. New York: IEEE. 2006. 78-86.
- [31] Kowsary F., Noroozi N. and Rezaei Barmi M. Optimization of Heat Transfer Rate in the Rectangular Microchannel of Different Aspect Ratios With Constant Cross Sectional Area. *ASME 2008 First International Conference on Micro/Nanoscale Heat Transfer.* June 6-9, 2008. New York: ASME. 2009. 285-92.
- [32] Sobhan C. B., Anoop P. S., Arimboor K., Abraham T. and Peterson G. P. Microchannel Optimization for Heat Dissipation From a Solid Substrate. *ASME 2008 First International Conference on Micro/Nanoscale Heat Transfer.* June 6-9, 2008. New York: ASME. 2009. 671-7.

- [33] Kou H.-S., Lee J.-J. and Chen C.-W. Optimum thermal performance of microchannel heat sink by adjusting channel width and height. *Int Commun Heat Mass Transfer*. 2008. 35(5): 577-82.
- [34] Chong S., Ooi K. and Wong T. Optimisation of single and double layer counter flow microchannel heat sinks. *Appl Therm Eng*. 2002. 22(14): 1569-85.
- [35] Wei X. and Joshi Y. Optimization study of stacked micro-channel heat sinks for micro-electronic cooling. *IEEE Trans Compon Packag Technol*. 2003. 26(1): 55-61.
- [36] Hung T.-C. and Yan W.-M. Optimization of a microchannel heat sink with varying channel heights and widths. *Numerical Heat Transfer, Part A: Applications*. 2012. 62(9): 722-41.
- [37] Wang T.-H., Wu H.-C., Meng J.-H. and Yan W.-M. Optimization of a double-layered microchannel heat sink with semi-porous-ribs by multi-objective genetic algorithm. *Int J Heat Mass Transfer*. 2020. 149: 119217.
- [38] Beng S. W. and Japar W. M. A. A. Numerical analysis of heat and fluid flow in microchannel heat sink with triangular cavities. *J Adv Res Fluid Mech Therm Sci*. 2017. 34(1): 1-8.
- [39] van Erp R., Soleimanzadeh R., Nela L., Kampitsis G. and Matioli E. Co-designing electronics with microfluidics for more sustainable cooling. *Nature*. 2020. 585(7824): 211-6.
- [40] Lu H., Xu M., Gong L., Duan X. and Chai J. C. Effects of surface roughness in microchannel with passive heat transfer enhancement structures. *Int J Heat Mass Transfer*. 2020. 148: 119070.
- [41] Yan Y., Yan H., Yin S., Zhang L. and Li L. Single/multi-objective optimizations on hydraulic and thermal management in micro-channel heat sink with bionic Y-shaped fractal network by genetic algorithm coupled with numerical simulation. *International Journal of Heat and Mass Transfer*. 2019. 129: 468-79.
- [42] Naquiuddin N. H., Saw L. H., Yew M. C., Yusof F., Poon H. M., Cai Z. and Thiam H. S. Numerical investigation for optimizing segmented micro-channel heat sink by Taguchi-Grey method. *Applied Energy*. 2018. 222: 437-50.
- [43] Li Y., Xia G., Ma D., Jia Y. and Wang J. Characteristics of laminar flow and heat transfer in microchannel heat sink with triangular cavities and rectangular ribs. *Int J Heat Mass Transfer*. 2016. 98: 17-28.

- [44] Rajalingam A. and Chakraborty S. Estimation of the thermohydraulic performance of a microchannel heat sink with gradual and sudden variation of the flow passage. *Int J Heat Mass Transfer*. 2022. 190: 122776.
- [45] Zhu Q., Su R., Xia H., Zeng J. and Chen J. Numerical simulation study of thermal and hydraulic characteristics of laminar flow in microchannel heat sink with water droplet cavities and different rib columns. *Int J Therm Sci*. 2022. 172(Part B): 107319.
- [46] Bayrak E., Olcay A. B. and Serincan M. F. Numerical investigation of the effects of geometric structure of microchannel heat sink on flow characteristics and heat transfer performance. *Int J Therm Sci*. 2019. 135: 589-600.
- [47] Zhu Q., Jin Y., Chen J., Su R., Zhu F., Li H., Wan J., Zhang H., Sun H. and Cui Y. Computational study of rib shape and configuration for heat transfer and fluid flow characteristics of microchannel heat sinks with fan-shaped cavities. *Appl Therm Eng*. 2021. 195: 117171.
- [48] Gong L. and Wei B. The characteristics of fluid flow and heat transfer in wavy, dimple and wavy-dimple microchannels. *Applied Mechanics and Materials*. September, 2013. Switzerland: Trans Tech Publ. 2013. 173-8.
- [49] Li Y., Xia G., Jia Y., Ma D., Cai B. and Wang J. Effect of geometric configuration on the laminar flow and heat transfer in microchannel heat sinks with cavities and fins. *Numerical Heat Transfer, Part A: Applications*. 2017. 71(5): 528-46.
- [50] Ghani I. A., Kamaruzaman N. and Sidik N. A. C. Heat transfer augmentation in a microchannel heat sink with sinusoidal cavities and rectangular ribs. *Int J Heat Mass Transfer*. 2017. 108(Part B): 1969-81.
- [51] Liu X., Zhang H., Wang F., Zhu C., Li Z., Zhao D., Jiang H., Liu Y. and Zhang Z. Thermal and hydraulic performances of the wavy microchannel heat sink with fan-shaped ribs on the sidewall. *Int J Therm Sci*. 2022. 179: 107688.
- [52] Ahmad F., Cheema T. A., Mohib Ur Rehman M., Ilyas M. and Park C. W. Thermodynamic analysis of microchannel heat sink with cylindrical ribs and cavities. *J Heat Transfer*. 2020. 142(9): 1-11.
- [53] Razali S., Sidik N. and Yusof S. Numerical studies of fluid flow and heat transfer in microchannel heat sink with trapezoidal cavities, ribs and secondary channel. *Journal of Physics: Conference Series*. October 1, 2021. United Kingdom: IOP Publishing. 2021. 012022.

- [54] Zhu Q., Chang K., Chen J., Zhang X., Xia H., Zhang H., Wang H., Li H. and Jin Y. Characteristics of heat transfer and fluid flow in microchannel heat sinks with rectangular grooves and different shaped ribs. *Alexandria Engineering Journal*. 2020. 59(6): 4593-609.
- [55] Sikdar P., Datta A., Biswas N. and Sanyal D. Identifying improved microchannel configuration with triangular cavities and different rib structures through evaluation of thermal performance and entropy generation number. *Phys Fluids*. 2020. 32(3): 033601.
- [56] Xia G., Zhai Y. and Cui Z. Characteristics of entropy generation and heat transfer in a microchannel with fan-shaped reentrant cavities and internal ribs. *Sci China Technol Sci*. 2013. 56(7): 1629-35.
- [57] Xie Y., Shen Z., Zhang D. and Lan J. Thermal performance of a water-cooled microchannel heat sink with grooves and obstacles. *J Electron Packag*. 2014. 136(2): 021001.
- [58] Naqiuddin N. H., Saw L. H., Yew M. C., Yusof F., Poon H. M., Cai Z. and San Thiam H. Numerical investigation for optimizing segmented micro-channel heat sink by Taguchi-Grey method. *Appl Energy*. 2018. 222: 437-50.
- [59] Liu L., Cao Z., Xu C., Zhang L. and Sun T. Investigation of fluid flow and heat transfer characteristics in a microchannel heat sink with double-layered staggered cavities. *Int J Heat Mass Transfer*. 2022. 187: 122535.
- [60] Go J. S. Design of a microfin array heat sink using flow-induced vibration to enhance the heat transfer in the laminar flow regime. *Sens Actuators, A*. 2003. 105(2): 201-10.
- [61] Yeom T., Simon T. W., Huang L., North M. T. and Cui T. Piezoelectric translational agitation for enhancing forced-convection channel-flow heat transfer. *Int J Heat Mass Transfer*. 2012. 55(25-26): 7398-409.
- [62] Yeom T., Simon T., Zhang M., Yu Y. and Cui T. Active heat sink with piezoelectric translational agitators, piezoelectric synthetic jets, and micro pin fin arrays. *Exp Therm Fluid Sci*. 2018. 99: 190-9.
- [63] Krishnaveni T., Renganathan T., Picardo J. and Pushpavanam S. Numerical study of enhanced mixing in pressure-driven flows in microchannels using a spatially periodic electric field. *Phys Rev E*. 2017. 96(3): 033117.
- [64] Hessami M.-A., Berryman A. and Bandopdhayay P. Heat Transfer Enhancement in an Electrically Heated Horizontal Pipe Due to Flow Pulsation.

- ASME 2003 International Mechanical Engineering Congress and Exposition*. November 15-21, 2003. USA: ASME. 2008. 49-56.
- [65] Zhang H., Li S., Cheng J., Zheng Z., Li X. and Li F. Numerical study on the pulsating effect on heat transfer performance of pseudo-plastic fluid flow in a manifold microchannel heat sink. *Appl Therm Eng*. 2018. 129: 1092-105.
- [66] Wang C.-S., Wei T.-C., Shen P.-Y. and Liou T.-M. Lattice Boltzmann study of flow pulsation on heat transfer augmentation in a louvered microchannel heat sink. *Int J Heat Mass Transfer*. 2020. 148: 119139.
- [67] Shen S., Xu J., Zhou J. and Chen Y. Flow and heat transfer in microchannels with rough wall surface. *Energy Convers Manage*. 2006. 47(11-12): 1311-25.
- [68] Jones B. J. and Garimella S. V. Surface roughness effects on flow boiling in microchannels. *J Therm Sci Eng Appl*. 2009. 1(4): 041007.
- [69] Gulbe L., Jekabsons N. and Traskovs A. Parametric studies for vertical axis wind turbine simulations. *Environmental and Climate Technologies*. 2011. 6(1): 23-30.
- [70] Alam T., Lee P. S. and Yap C. R. Effects of surface roughness on flow boiling in silicon microgap heat sinks. *International Journal of Heat and Mass Transfer*. 2013. 64: 28-41.
- [71] MA T. Effects of Surface Roughness on Thermal and Hydrodynamic Behaviors in Microchannel Using Lattice Boltzmann Method. *International Journal of Fluid Machinery and Systems*. 2017. 10(4): 439-46.
- [72] Javanbakht M.-H. and Moosavi A. Heat transfer on topographically structured surfaces for power law fluids. *Int J Heat Mass Transfer*. 2018. 121: 857-71.
- [73] Jing D., Song S., Pan Y. and Wang X. Size dependences of hydraulic resistance and heat transfer of fluid flow in elliptical microchannel heat sinks with boundary slip. *Int J Heat Mass Transfer*. 2018. 119: 647-53.
- [74] Hong F. and Cheng P. Three dimensional numerical analyses and optimization of offset strip-fin microchannel heat sinks. *Int Commun Heat Mass Transfer*. 2009. 36(7): 651-6.
- [75] Chai L., Xia G., Zhou M., Li J. and Qi J. Optimum thermal design of interrupted microchannel heat sink with rectangular ribs in the transverse microchambers. *Appl Therm Eng*. 2013. 51(1-2): 880-9.

- [76] Xie G., Zhang F., Sundén B. and Zhang W. Constructal design and thermal analysis of microchannel heat sinks with multistage bifurcations in single-phase liquid flow. *Applied thermal engineering*. 2014. 62(2): 791-802.
- [77] Kamal H. and Dewan A. Analysis of interrupted rectangular microchannel heat sink with high aspect ratio. *J Appl Fluid Mech*. 2017. 10(1): 117-26.
- [78] Chai L. and Wang L. Thermal-hydraulic performance of interrupted microchannel heat sinks with different rib geometries in transverse microchambers. *Int J Therm Sci*. 2018. 127: 201-12.
- [79] Mario Di Capua H., Escobar R., Diaz A. and Guzmán A. M. Enhancement of the cooling capability of a high concentration photovoltaic system using microchannels with forward triangular ribs on sidewalls. *Appl Energy*. 2018. 226: 160-80.
- [80] Saravanan V. and Umesh C. Numerical comparison for thermo-hydraulic performance of pin fin heat sink with micro channel pin fin heat sink. *Sādhanā*. 2018. 43(7): 100.
- [81] Shen H., Liu X., Yan H., Xie G. and Sunden B. Enhanced thermal performance of internal y-shaped bifurcation microchannel heat sinks with metal foams. *J Therm Sci Eng Appl*. 2018. 10(1): 011001.
- [82] Ming T., Cai C., Yang W., Shen W. and Gan T. Optimization of dimples in microchannel heat sink with impinging jets—Part A: mathematical model and the influence of dimple radius. *J Therm Sci*. 2018. 27(3): 195-202.
- [83] Sui Y., Teo C., Lee P. S., Chew Y. and Shu C. Fluid flow and heat transfer in wavy microchannels. *Int J Heat Mass Transfer*. 2010. 53(13-14): 2760-72.
- [84] Mills Z. G., Waley A. and Alexeev A. Heat transfer enhancement and thermal-hydraulic performance in laminar flows through asymmetric wavy walled channels. *Int J Heat Mass Transfer*. 2016. 97: 450-60.
- [85] Lin L., Zhao J., Lu G., Wang X.-D. and Yan W.-M. Heat transfer enhancement in microchannel heat sink by wavy channel with changing wavelength/amplitude. *International Journal of Thermal Sciences*. 2017. 118: 423-34.
- [86] Hasis F. B. A., Krishna P. M., Aravind G., Deepu M. and Shine S. Thermo hydraulic performance analysis of twisted sinusoidal wavy microchannels. *Int J Therm Sci*. 2018. 128: 124-36.

- [87] Parlak Z. Optimal design of wavy microchannel and comparison of heat transfer characteristics with zigzag and straight geometries. *Heat and Mass Transfer*. 2018. 54(11): 3317-28.
- [88] Ermagan H. and Rafee R. Numerical investigation into the thermo-fluid performance of wavy microchannels with superhydrophobic walls. *Int J Therm Sci*. 2018. 132: 578-88.
- [89] Kuppusamy N. R. *Thermal enhancement in a microchannel heat sink using passive methods*. Ph.D. Thesis. University of Malaya; 2016.
- [90] Deng D., Xie Y., Huang Q. and Wan W. On the flow boiling enhancement in interconnected reentrant microchannels. *Int J Heat Mass Transfer*. 2017. 108(Part A): 453-67.
- [91] Lee Y. J., Lee P. S. and Chou S. K. Enhanced Thermal Transport in Microchannel Using Oblique Fins. *J Heat Transfer*. 2012. 134(10): 101901.
- [92] Kuppusamy N. R., Saidur R., Ghazali N. and Mohammed H. Numerical study of thermal enhancement in micro channel heat sink with secondary flow. *Int J Heat Mass Transfer*. 2014. 78: 216-23.
- [93] Law M., Lee P.-S. and Balasubramanian K. Experimental investigation of flow boiling heat transfer in novel oblique-finned microchannels. *Int J Heat Mass Transfer*. 2014. 76: 419-31.
- [94] Lee Y. J., Singh P. K. and Lee P. S. Fluid flow and heat transfer investigations on enhanced microchannel heat sink using oblique fins with parametric study. *International Journal of Heat and Mass Transfer*. 2015. 81: 325-36.
- [95] Law M. and Lee P.-S. A comparative study of experimental flow boiling heat transfer and pressure characteristics in straight-and oblique-finned microchannels. *Int J Heat Mass Transfer*. 2015. 85: 797-810.
- [96] Law M., Kanargi O. B. and Lee P.-S. Effects of varying oblique angles on flow boiling heat transfer and pressure characteristics in oblique-finned microchannels. *Int J Heat Mass Transfer*. 2016. 100: 646-60.
- [97] Law M. and Lee P.-S. Effects of varying secondary channel widths on flow boiling heat transfer and pressure characteristics in oblique-finned microchannels. *Int J Heat Mass Transfer*. 2016. 101: 313-26.
- [98] Viktorov V., Mahmud M. R. and Visconte C. Design and characterization of a new HC passive micromixer up to Reynolds number 100. *Chem Eng Res Des*. 2016. 108: 152-63.

- [99] Sivashankar S., Agambayev S., Mashraei Y., Li E. Q., Thoroddsen S. T. and Salama K. N. A “twisted” microfluidic mixer suitable for a wide range of flow rate applications. *Biomicrofluidics*. 2016. 10(3): 034120.
- [100] Huanming X., Jiawei W. and Zhiping W. A comparative discussion of different designs of passive micromixers: specific sensitivities of mixing efficiency on Reynolds numbers and fluid properties. *Microsyst Technol*. 2018. 24(2): 1253-63.
- [101] Hayashi Y., Saneie N., Yip G., Kim Y. J. and Kim J.-H. Metallic nanoemulsion with galinstan for high heat-flux thermal management. *Int J Heat Mass Transfer*. 2016. 101: 1204-16.
- [102] Xia G., Liu R., Wang J. and Du M. The characteristics of convective heat transfer in microchannel heat sinks using Al₂O₃ and TiO₂ nanofluids. *Int Commun Heat Mass Transfer*. 2016. 76: 256-64.
- [103] Wu J., Zhao J., Lei J. and Liu B. Effectiveness of nanofluid on improving the performance of microchannel heat sink. *Appl Therm Eng*. 2016. 101: 402-12.
- [104] Rabby M. I. I., Masuri S. U., Kaniappan L., Loulou T. and Sadrul A. Effect of Water Based Nanofluids on Laminar Convective Heat Transfer in Developing Region of Rectangular Channel. *CFD Lett*. 2019. 11(12): 74-87.
- [105] Japar W. M. A. A., Sidik N. A. C., Saidur R., Asako Y. and Mohd M. I. Temperature Minimization on the Substrate of a Heat Sink By Rib-Groove Microchannel Heat Sink with Effective Energy Consumption: Groove Geometry Parameter Effects. *CFD Lett*. 2019. 11(9): 1-13.
- [106] Japar W. M. A. A., Sidik N. A. C., Saidur R., Asako Y. and Yusof S. N. A. A review of passive methods in microchannel heat sink application through advanced geometric structure and nanofluids: Current advancements and challenges. *Nanotechnology Reviews*. 2020. 9(1): 1192-216.
- [107] Bhandari P. and Prajapati Y. K. Thermal performance of open microchannel heat sink with variable pin fin height. *Int J Therm Sci*. 2021. 159: 106609.
- [108] Yuan D., Zhou W., Fu T. and Liu C. Experimental and numerical investigation of heat and mass transfer in non-uniform wavy microchannels. *Int J Therm Sci*. 2020. 152: 106320.
- [109] Li P., Luo Y., Zhang D. and Xie Y. Flow and heat transfer characteristics and optimization study on the water-cooled microchannel heat sinks with dimple and pin-fin. *Int J Heat Mass Transfer*. 2018. 119: 152-62.

- [110] Gong L., Lu H., Li H. and Xu M. Parametric numerical study of the flow and heat transfer in a dimpled wavy microchannel. *Heat Transf Res.* 2016. 47(2): 105-18.
- [111] Srivastava P., Dewan A. and Bajpai J. K. Flow and heat transfer characteristics in convergent-divergent shaped microchannel with ribs and cavities. *Int J Heat Technol.* 2017. 35(4): 863-73.
- [112] Xia G., Jia Y., Li Y., Ma D. and Cai B. Numerical simulation and multiobjective optimization of a microchannel heat sink with arc-shaped grooves and ribs. *Numerical Heat Transfer, Part A: Applications.* 2016. 70(9): 1041-55.
- [113] Biswal P. and Basak T. Entropy generation vs energy efficiency for natural convection based energy flow in enclosures and various applications: A review. *Renewable Sustainable Energy Rev.* 2017. 80: 1412-57.
- [114] Ghani I. A., Sidik N. A. C., Mamat R., Najafi G., Ken T. L., Asako Y. and Japar W. M. A. A. Heat transfer enhancement in microchannel heat sink using hybrid technique of ribs and secondary channels. *International Journal of Heat and Mass Transfer.* 2017. 114: 640-55.
- [115] Huang X., Yang W., Ming T., Shen W. and Yu X. Heat transfer enhancement on a microchannel heat sink with impinging jets and dimples. *Int J Heat Mass Transfer.* 2017. 112: 113-24.
- [116] Ming T., Cai C., Yang W., Shen W., Feng W. and Zhou N. Optimization of dimples in microchannel heat sink with impinging jets—part B: the influences of dimple height and arrangement. *J Therm Sci.* 2018. 27(4): 321-30.
- [117] Bahiraei M., Jamshidmofid M. and Goodarzi M. Efficacy of a hybrid nanofluid in a new microchannel heat sink equipped with both secondary channels and ribs. *J Mol Liq.* 2019. 273: 88-98.
- [118] Wang R.-j., Wang J.-w., Lijin B.-q. and Zhu Z.-f. Parameterization investigation on the microchannel heat sink with slant rectangular ribs by numerical simulation. *Appl Therm Eng.* 2018. 133: 428-38.
- [119] Ansari D. and Kim K.-Y. Hotspot thermal management using a microchannel-pinfin hybrid heat sink. *Int J Therm Sci.* 2018. 134: 27-39.
- [120] Japar W. M. A. A., Sidik N. A. C. and Mat S. A comprehensive study on heat transfer enhancement in microchannel heat sink with secondary channel. *International Communications in Heat and Mass Transfer.* 2018. 99: 62-81.

- [121] Xie G., Li Y., Zhang F. and Sundén B. Analysis of micro-channel heat sinks with rectangular-shaped flow obstructions. *Numerical Heat Transfer, Part A: Applications*. 2016. 69(4): 335-51.
- [122] Yang M., Li M.-T., Hua Y.-C., Wang W. and Cao B.-Y. Experimental study on single-phase hybrid microchannel cooling using HFE-7100 for liquid-cooled chips. *Int J Heat Mass Transfer*. 2020. 160: 120230.
- [123] Li Y., Wang Z., Yang J. and Liu H. Thermal and hydraulic characteristics of microchannel heat sinks with cavities and fins based on field synergy and thermodynamic analysis. *Appl Therm Eng*. 2020. 175: 115348.
- [124] Japar W. M. A. A., Sidik N. A. C., Saidur R., Kamaruzaman N., Asako Y. and Yusof S. N. A. The Effect of Triangular Cavity Shape on the Hybrid Microchannel Heat Sink Performance. *CFD Lett*. 2020. 12(9): 1-14.
- [125] Japar W., Sidik N., Saidur R., Asako Y. and Muhammad N. Thermal Performance Analysis in Sinusoidal-Cavities-Ribs Microchannel Heat Sink with Secondary Channel Geometry for Low Pumping Power Application. *IOP Conference Series: Materials Science and Engineering*. July 1, 2020. United Kingdom: IOP Publishing. 2020. 012087.
- [126] Japar W. M. A. A., Sidik N. A. C. and Asako Y. Entropy Generation Minimization In Sinusoidal Cavities-Ribs Microchannel Heat Sink Via Secondary Channel Geometry. *CFD Lett*. 2019. 11(7): 1-10.
- [127] Japar W. M. A. A. and Sidik N. A. C. The effectiveness of secondary channel on the performance of hybrid microchannel heat sink at low pumping power. *IOP Conference Series: Materials Science and Engineering*. January 16, 2019. United Kingdom: IOP Publishing. 2019. 012032.
- [128] Japar W. M. A. A. and Sidik N. A. C. *Hybrid Microchannel Heat Sink with Secondary Channel Geometry (TC-RR-SC MCHS)*. AR2019002047. 2019
- [129] Choi S. U. and Eastman J. A. Enhancing thermal conductivity of fluids with nanoparticles. *International mechanical engineering congress and exhibition*. November 12-17, 1995. United States: Argonne National Lab., IL (United States). 1995. 2-8.
- [130] Lyu Z. J., Asadi A., Alarifi I. M., Ali V. and Foong L. K. Thermal and Fluid Dynamics Performance of MWCNT-Water Nanofluid Based on Thermophysical Properties: An Experimental and Theoretical Study. *Sci Rep*. 2020. 10(1): 14.

- [131] Xian H. W., Sidik N. A. C. and Saidur R. Impact of different surfactants and ultrasonication time on the stability and thermophysical properties of hybrid nanofluids. *Int Commun Heat Mass Transfer*. 2020. 110: 104389.
- [132] Sidik N. A. C., Jamil M. M., Japar W. M. A. A. and Adamu I. M. A review on preparation methods, stability and applications of hybrid nanofluids. *Renewable and Sustainable Energy Reviews*. 2017. 80: 1112-22.
- [133] Abubakar S., Azwadi C. N. and Ahmad A. The use of Fe₃O₄-H₂O₄ nanofluid for heat transfer enhancement in rectangular microchannel heatsink. *J Adv Res Mater Sci*. 2016. 23(1): 15-24.
- [134] Sivakumar A., Alagumurthi N. and Senthilvelan T. Effect of serpentine grooves on heat transfer characteristics of microchannel heat sink with different nanofluids. *Heat Transfer—Asian Research*. 2017. 46(3): 201-17.
- [135] Snoussi L., Ouerfelli N., Sharma K., Vranceanu N., Chamkha A. and Guizani A. Numerical simulation of nanofluids for improved cooling efficiency in a 3D copper microchannel heat sink (MCHS). *Phys Chem Liq*. 2018. 56(3): 311-31.
- [136] Sarafraz M., Nikkhah V., Nakhjavani M. and Arya A. Fouling formation and thermal performance of aqueous carbon nanotube nanofluid in a heat sink with rectangular parallel microchannel. *Appl Therm Eng*. 2017. 123: 29-39.
- [137] Thansekhar M. and Anbumeenakshi C. Experimental investigation of thermal performance of microchannel heat sink with nanofluids Al₂O₃/water and SiO₂/water. *Exp Tech*. 2017. 41(4): 399-406.
- [138] Arani A. A. A., Akbari O. A., Safaei M. R., Marzban A., Alrashed A. A., Ahmadi G. R. and Nguyen T. K. Heat transfer improvement of water/single-wall carbon nanotubes (SWCNT) nanofluid in a novel design of a truncated double-layered microchannel heat sink. *Int J Heat Mass Transfer*. 2017. 113: 780-95.
- [139] Duangthongsuk W. and Wongwises S. An experimental investigation on the heat transfer and pressure drop characteristics of nanofluid flowing in microchannel heat sink with multiple zigzag flow channel structures. *Exp Therm Fluid Sci*. 2017. 87: 30-9.
- [140] Vinoth R. and Kumar D. S. Channel cross section effect on heat transfer performance of oblique finned microchannel heat sink. *Int Commun Heat Mass Transfer*. 2017. 87: 270-6.

- [141] Abdollahi A., Sharma R. N., Mohammed H. A. and Vatani A. Heat transfer and flow analysis of Al₂O₃-Water nanofluids in interrupted microchannel heat sink with ellipse and diamond ribs in the transverse microchambers. *Heat Transfer Eng.* 2018. 39(16): 1461-9.
- [142] ALFARYJAT A., GHEORGHIAN A.-T., NABBAT A., ȘTEFĂNESCU M.-F. and DOBROVICESCU A. The Impact of Different Base Nanofluids on the Fluid Flow and Heat Transfer Characteristics in Rhombus Microchannels Heat Sink. *Scientific Bulletin, Series D.* 2018. 80(1): 1-14.
- [143] Sarafraz M., Nikkhah V., Nakhjavani M. and Arya A. Thermal performance of a heat sink microchannel working with biologically produced silver-water nanofluid: experimental assessment. *Exp Therm Fluid Sci.* 2018. 91: 509-19.
- [144] Arabpour A., Karimipour A. and Toghraie D. The study of heat transfer and laminar flow of kerosene/multi-walled carbon nanotubes (MWCNTs) nanofluid in the microchannel heat sink with slip boundary condition. *J Therm Anal Calorim.* 2018. 131(2): 1553-66.
- [145] Tran N., Chang Y.-J. and Wang C.-C. Optimization of thermal performance of multi-nozzle trapezoidal microchannel heat sinks by using nanofluids of Al₂O₃ and TiO₂. *Int J Heat Mass Transfer.* 2018. 117: 787-98.
- [146] Lyu Z. J., Pourfattah F., Arani A. A. A., Asadi A. and Foong L. K. On the Thermal Performance of a Fractal Microchannel Subjected to Water and Kerosene Carbon Nanotube Nanofluid. *Sci Rep.* 2020. 10(1): 16.
- [147] Razali A., Sadikin A. and Ibrahim S. Heat transfer of Al₂O₃ nanofluids in microchannel heat sink. *AIP Conference Proceedings.* Apr 21, 2017. USA: AIP Publishing LLC. 2017. 020050.
- [148] Chabi A., Zarrinabadi S., Peyghambarzadeh S., Hashemabadi S. and Salimi M. Local convective heat transfer coefficient and friction factor of CuO/water nanofluid in a microchannel heat sink. *Heat and Mass Transfer.* 2017. 53(2): 661-71.
- [149] Manay E. and Sahin B. Heat transfer and pressure drop of nanofluids in a microchannel heat sink. *Heat Transfer Eng.* 2017. 38(5): 510-22.
- [150] Gilmore N., Timchenko V. and Menictas C. Manifold microchannel heat sink topology optimisation. *Int J Heat Mass Transfer.* 2021. 170: 121025.

- [151] Ozguc S., Pan L. and Weibel J. A. Topology optimization of microchannel heat sinks using a homogenization approach. *Int J Heat Mass Transfer*. 2021. 169: 120896.
- [152] Zhou J., Hu M. and Jing D. An efficient method for the geometric parameters optimization of double-layer micro-channel heat sink. *Numerical Heat Transfer, Part A: Applications*. 2020. 77(11): 966-80.
- [153] Tartibu Kwanda L. Multi-objective optimization of a rectangular micro-channel heat sink using the augmented ϵ -constraint method. *Engineering Optimization*. 2020. 52(1): 22-36.
- [154] Yang M. and Cao B.-Y. Multi-objective optimization of a hybrid microchannel heat sink combining manifold concept with secondary channels. *Appl Therm Eng*. 2020. 181: 115592.
- [155] Alfellag M. A., Ahmed H. E., Fadhil O. T. and Kherbeet A. S. Optimal hydrothermal design of microchannel heat sink using trapezoidal cavities and solid/slotted oval pins. *Appl Therm Eng*. 2019. 158: 113765.
- [156] Shi X., Li S., Mu Y. and Yin B. Geometry parameters optimization for a microchannel heat sink with secondary flow channel. *Int Commun Heat Mass Transfer*. 2019. 104: 89-100.
- [157] Alfellag M. A., Ahmed H. E. and Kherbeet A. S. Numerical simulation of hydrothermal performance of minichannel heat sink using inclined slotted plate-fins and triangular pins. *Appl Therm Eng*. 2020. 164: 114509.
- [158] Pourhammati S. and Hossainpour S. Improving the hydrothermal characteristics of wavy microchannel heat sink by modification of wavelength and wave amplitude. *Int Commun Heat Mass Transfer*. 2022. 130: 105805.
- [159] Sun L., Li J., Xu H., Ma J. and Peng H. Numerical study on heat transfer and flow characteristics of novel microchannel heat sinks. *Int J Therm Sci*. 2022. 176: 107535.
- [160] Zhang F., Wu B. and Du B. Heat transfer optimization based on finned microchannel heat sink. *Int J Therm Sci*. 2022. 172(Part B): 107357.
- [161] Zhu Q., Zhu F., Fu D., Zhang A. and Zhang S. Effects of geometric parameters on fluid flow and heat transfer in microchannel heat sink with trapezoidal grooves in sidewalls. *Thermal Science*. 2022. 2022(00): 49-.

- [162] Kumar K., Kumar R. and Bharj R. S. Circular Microchannel Heat Sink Optimization Using Entropy Generation Minimization Method. *Journal of Non-Equilibrium Thermodynamics*. 2020. 45(4): 333-42.
- [163] Subrahmanyam K. B., Datta A. and Das P. Parametric study of heat transfer performance including entropy generation of microchannel heat sink with fan cavity and different rib structure. *Proceedings of the Institution of Mechanical Engineers, Part E: Journal of Process Mechanical Engineering*. 2022. 236(2): 368-82.
- [164] Patel H. and Matawala V. Performance Evaluation and parametric optimization of a Heat Sink for Cooling of Electronic Devices with Entropy Generation Minimization. *European Journal of Sustainable Development Research*. 2019. 3(4): em0100.
- [165] Phillips R. J. Microchannel heat sinks. *Advances in Thermal Modeling of Electronic Components*. 1990. 1(1): 31-48.
- [166] Shah R. K. and London A. L. Laminar flow forced convection heat transfer and flow friction in straight and curved ducts-a summary of analytical solutions: Stanford Univ CA Dept of Mechanical Engineering 1971.
- [167] Wang G., Qian N. and Ding G. Heat transfer enhancement in microchannel heat sink with bidirectional rib. *Int J Heat Mass Transfer*. 2019. 136: 597-609.
- [168] Chang S.-W., Sadeghianjahromi A., Sheu W.-J. and Wang C.-C. Numerical study of oblique fins under natural convection with experimental validation. *Int J Therm Sci*. 2022. 179: 107668.
- [169] Hua J., Hou W., Li G., Qin L., Li D. and Zhao X. The experimental study on the boiling bubble behaviors and heat transfer performance of the deionized water across various pin fins. *Heat and Mass Transfer*. 2021. 57(10): 1609-22.
- [170] Sun R., Hua J., Zhang X. and Zhao X. Experimental study on the effect of shape on the boiling flow and heat transfer characteristics of different pin-fin microchannels. *Heat and Mass Transfer*. 2021. 57(12): 2081-95.
- [171] Phillips R. J. Microchannel heat sinks. *Advances in thermal modeling of electronic components and systems*. 1990. 2: 109-84.
- [172] Steinke M. E. and Kandlikar S. G. Single-phase heat transfer enhancement techniques in microchannel and minichannel flows. *Second International Conference on Microchannels and Minichannels, Rochester, NY, June*. 17-9.

- [173] Han C.-L., Ren J.-J., Dong W.-P. and Bi M.-S. Numerical investigation of supercritical LNG convective heat transfer in a horizontal serpentine tube. *Cryogenics*. 2016. 78: 1-13.
- [174] Hua Y.-X., Wang Y.-Z. and Meng H. A numerical study of supercritical forced convective heat transfer of n-heptane inside a horizontal miniature tube. *J Supercrit Fluids*. 2010. 52(1): 36-46.
- [175] Wang Y.-Z., Hua Y.-X. and Meng H. Numerical studies of supercritical turbulent convective heat transfer of cryogenic-propellant methane. *J Thermophys Heat Transfer*. 2010. 24(3): 490-500.
- [176] CATIA. CATIAV5R20. Dassault Systems, USA. 1998. <https://www.3ds.com/>.
- [177] ANSYS. ANSYS 17.0. ANSYS, Inc, USA. 2016. <https://www.ansys.com/>.
- [178] TECPLOT360. Tecplot 360 EX 2017 R2. Tecplot, Inc, USA. 2017. <https://www.tecplot.com/>.
- [179] Technologies P. A. a. D. *ANSYS Meshing Advanced Techniques*. United States, 2016 ANSYS, Inc. 2017.
- [180] Guo J., Xu M. and Cheng L. Second law analysis of curved rectangular channels. *International Journal of Thermal Sciences*. 2011. 50(5): 760-8.
- [181] Rahmati A. R., Akbari O. A., Marzban A., Toghraie D., Karimi R. and Pourfattah F. Simultaneous investigations the effects of non-Newtonian nanofluid flow in different volume fractions of solid nanoparticles with slip and no-slip boundary conditions. *Thermal Science and Engineering Progress*. 2018. 5: 263-77.
- [182] Alrashed A. A., Akbari O. A., Heydari A., Toghraie D., Zarringhalam M., Shabani G. A. S., Seifi A. R. and Goodarzi M. The numerical modeling of water/FMWCNT nanofluid flow and heat transfer in a backward-facing contracting channel. *Physica B: Condensed Matter*. 2018. 537: 176-83.
- [183] Khodabandeh E., Rozati S. A., Joshaghani M., Akbari O. A., Akbari S. and Toghraie D. Thermal performance improvement in water nanofluid/GNP-SDBS in novel design of double-layer microchannel heat sink with sinusoidal cavities and rectangular ribs. *Journal of Thermal Analysis and Calorimetry*. 2018.
- [184] Bejan A. Second-Law Analysis in Heat Transfer and Thermal Design. In: Hartnett J. P. and Irvine T. F. *Advances in Heat Transfer*. New York: Elsevier. 1-58; 1982.

- [185] Bejan A. *Entropy Generation Minimization*, CRC Press. 1996.
- [186] Harouni H. G. *Investigation of chaotic advection regime and its effect on thermal performance of wavy walled microchannels*. Ph.D. Thesis. National University of Singapore; 2015.
- [187] Rohsenow W. M., Hartnett J. P. and Cho Y. I. *Handbook of heat transfer*. New York: McGraw-Hill. 1998.
- [188] Coleman H. W. and Steele W. G. *Experimentation, validation, and uncertainty analysis for engineers*. 4th ed. USA: John Wiley & Sons. 2018.
- [189] Japar W. M. A. A., Sidik N. A. C. and Beriache M. h. Hydrothermal Performance in a New Designed Hybrid Micro channel Heat Sink with Optimum Secondary Channel Geometry Parameter: Numerical and Experimental Studies. *Journal of Advanced Research Design*. 2019. 54(1): 13-27.
- [190] Cengel Y. A. *Fluid mechanics*. New York: Tata McGraw-Hill Education. 2010.
- [191] Ge Y., Liu Z. and Liu W. Multi-objective genetic optimization of the heat transfer for tube inserted with porous media. *Int J Heat Mass Transfer*. 2016. 101: 981-7.

LIST OF PUBLICATIONS

Journal with Impact Factor

1. **Japar W. M. A. A.**, Sidik N. A. C., Saidur R., Asako Y. and Yusof S. N. A. A review of passive methods in microchannel heat sink application through advanced geometric structure and nanofluids: Current advancements and challenges. *Nanotechnology Reviews*. 2020. 9(1): 1192-216. <https://doi.org/10.1515/ntrev-2020-0094>. (Q1, IF: 7.848)
2. **Japar W. M. A. A.**, Sidik N. A. C. and Mat S. A. Comprehensive study on heat transfer enhancement in microchannel heat sink with secondary channel. *Int Commun Heat Mass Transfer*. 2018. 99: 62-81. <https://doi.org/10.1016/j.icheatmasstransfer.2018.10.005>. (Q1, IF: 4.127)
3. Sidik N. A. C., Muhamad M. N. A. W., **Japar W. M. A. A.** and Rasid Z. A. An overview of passive techniques for heat transfer augmentation in microchannel heat sink. *Int Commun Heat Mass Transfer*. 2017. 88: 74-83. <https://doi.org/10.1016/j.icheatmasstransfer.2017.08.009>. (Q1, IF: 4.127)

Indexed Journal

1. **Japar W. M. A. A.**, Sidik N. A. C., Saidur R., Kamaruzaman N., Asako Y., Yusof S. N. A. and Lani M. N. Hybrid Microchannel Heat Sink with Sustainable Cooling Solutions: Numerical Model Validation. *CFD Lett*. 2022. 14(4): 91-117. (Indexed by SCOPUS)
2. **Japar W. M. A. A.**, Sidik N. A. C., Aid S. R., Asako Y. and Ken T. L. A comprehensive review on numerical and experimental study of nanofluid performance in microchannel heatsink (MCHS). *J Adv Res Fluid Mech Therm Sci*. 2018. 45(1): 165-76. (Indexed by SCOPUS)

Non-indexed Journal

1. **Japar W. M. A. A.**, Sidik N. A. C., Saidur R., Kamaruzaman N., Asako Y., Yusof S. N. A. and Lani M. N. Hybrid Microchannel Heat Sink with Sustainable Cooling Solutions: Experimental Analysis. *Journal of Advanced Research in Applied Mechanics*. 2022. 89(1): 1-6.
2. **Japar W. M. A. A.**, Sidik N. A. C., Kamaruzaman N., Asako Y., Muhammad N. M. a. Hydrothermal performance in the Hydrodynamic Entrance Region of Rectangular Microchannel Heat Sink. *Journal of Advanced Research in Numerical Heat Transfer*. 2020. 1(1): 22-31.

Patent/Copyright Publication

1. **Japar W. M. A. A.** and Sidik N. A. C. *Hybrid Microchannel Heat Sink with Secondary Channel Geometry (TC-RR-SC MCHS)*. AR2019002047. 2019.